

JET EVOLUTION VISUALIZED AND QUANTIFIED USING FILTERED RAYLEIGH SCATTERING

Mark F. Reeder
National Research Council Associate
NASA Lewis Research Center
Cleveland, Ohio

7-34
7-26/

Filtered Rayleigh scattering was utilized as a flow diagnostic in an investigation of a method of enhancing mixing in supersonic jets. The experiments were performed at the Aeronautical and Astronautical Research Laboratory at The Ohio State University. The primary objectives of the study were to visualize the effect of vortex-generating tabs on supersonic jets, to extract quantitative data from these planar visualizations, and to detect the presence of secondary flows (i.e. streamwise vorticity) generated by the tabs. An injection seeded frequency-doubled Nd:YAG was the light source and a 14-bit Princeton Instruments ICCD camera was used to record the image through an iodine cell. The incident wavelength of the laser was held constant for each flow case so that the filter absorbed unwanted background light, but permitted part of the thermally broadened Rayleigh scattered light to pass through. The visualizations were performed for axisymmetric jets ($D=1.9\text{cm}$) operated at perfectly expanded conditions for Mach 1.0, 1.5, and 2.0. All data was recorded for the jet cross-section at $x/D=3$. One hundred instantaneous images were recorded and averaged for each case, with a threshold set to eliminate unavoidable particulate scattering. A key factor in these experiments was that the stagnation air was heated such that the expansion of the flow in the nozzle resulted in the static temperature in the jet being equal to the ambient temperature, assuming isentropic flow. Since the thermodynamic conditions of the flow were approximately the same for each case, the increases in the intensity recorded by the ICCD camera could be directly attributed to the Doppler shift, and hence velocity. Visualizations were performed for Mach 1.5 and Mach 2.0 jets with tabs inserted at the nozzle exit. The distortion of the jet was readily apparent and was consistent with Mie scattering-based visualizations. Asymmetry in the intensities of the images indicate the presence of secondary flow patterns which are consistent the streamwise vortices measured using more traditional diagnostics in subsonic jets with the same tab configurations. Because each tab causes shocks to form, the assumption of isentropic flow is not valid for these cases. However, within a reasonable first-order estimation, the intensity across the illuminated plane for these cases can be related to a value combining density and velocity.

Goals of this work

- ☛ To visualize the effect of tabs on supersonic jets using filtered Rayleigh scattering (FRS).
- ☛ To extract quantitative data from the planar FRS visualizations.
- ☛ To detect secondary flows (i.e. streamwise vorticity) generated by tabs in supersonic jets.

TABLE 2. Flow characteristics for the FRS experiments.

D (cm)	P ₀ (MPa) (absolute)	T ₀ (K)	M _j	T _j (K)	ρ _j (kg/m ³)	U _j (m/s)	Re _D (*10 ⁶)	ρ _j /ρ _∞	M _c
1.90	0.1879	335	1.0	279	1.24	335	0.667	1.02	0.50
1.90	0.3647	400	1.5	276	1.25	499	0.992	1.03	0.75
1.90	0.7721	500	2.0	278	1.24	667	1.31	1.02	1.00

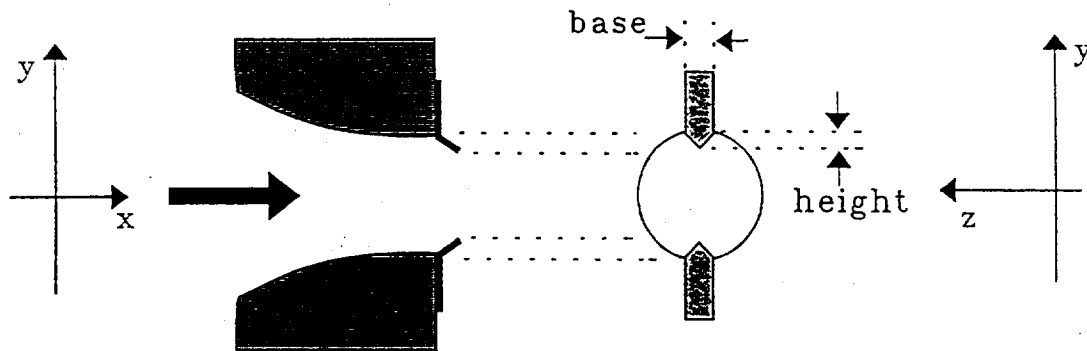


Figure 1. Sketch of a typical nozzle with two delta tabs. The base is 0.28D and the height is 0.10D for each tab.

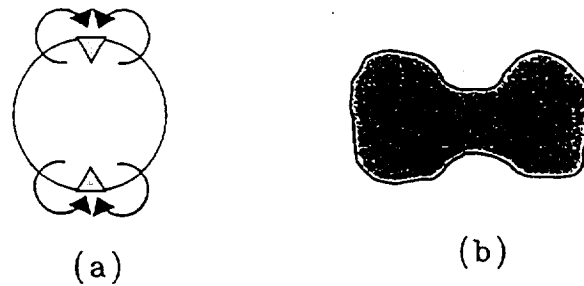


Figure 2. Sketch of (a) the direction of streamwise vortices generated by tabs, as measured in subsonic jets and (b) the resultant jet deformation caused by two delta tabs oriented as shown. [Zaman et. al. (1994)].

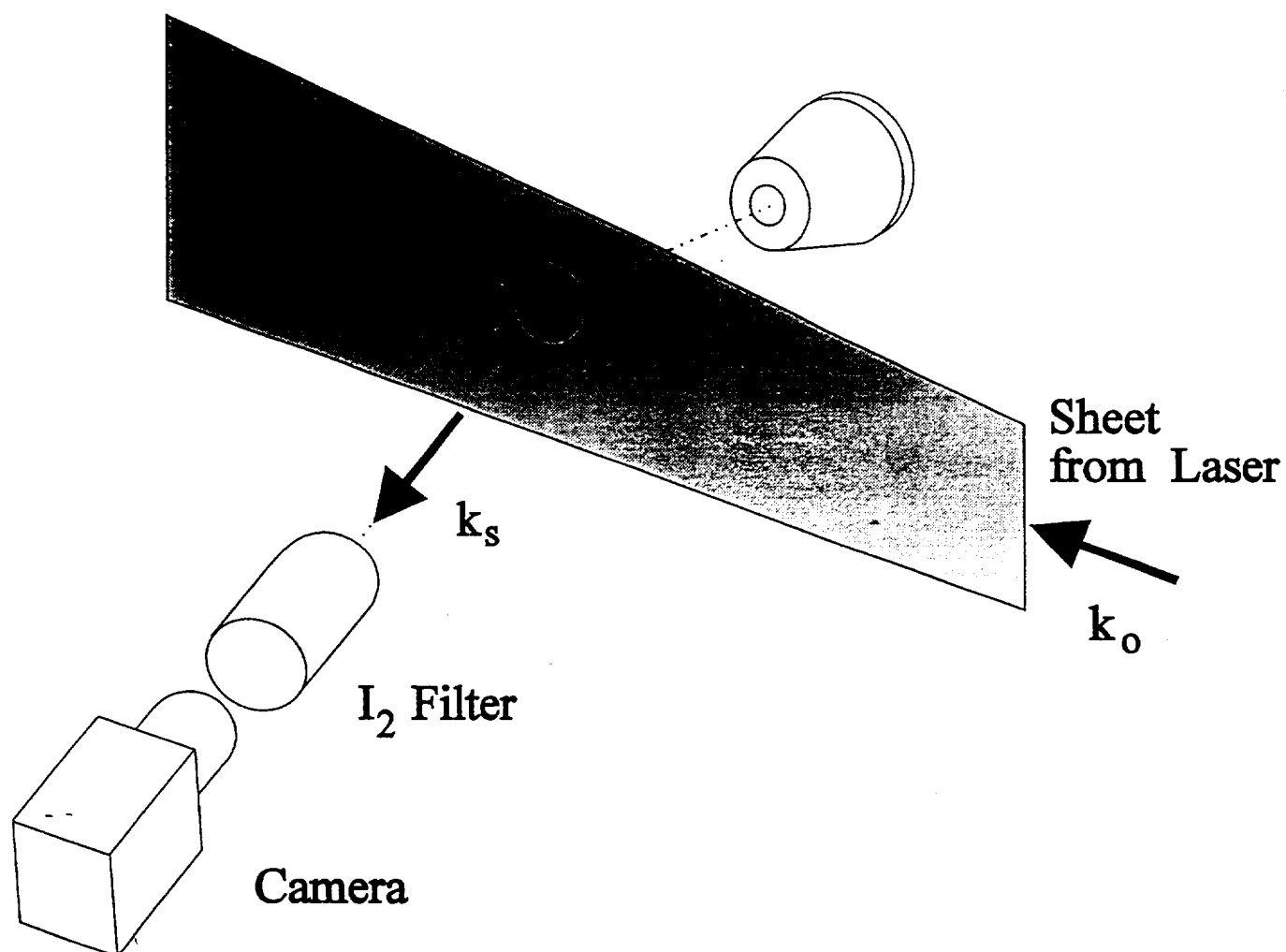


Figure 8. Sketch of the optical setup for the filtered Rayleigh scattering measurements in supersonic jets. The filter contains diatomic iodine in a gaseous state.

Density from unfiltered Rayleigh scattering may be described:

$$I = \rho \int_{f=-\infty}^{f=\infty} R^*(f) df \quad (1)$$

With a filter of known profile P_{filter} in the ambient air, where the directional velocity is zero:

$$I_{\infty} = \rho_{\infty} \int_{f=-\infty}^{f=\infty} [R^*(f_0, \rho_{\infty}, T_{\infty}, \theta)] [P_{filter}(f_0)] df \quad (2)$$

Due to the Doppler effect:

$$\Delta f = \frac{\bar{V}}{\lambda} \cdot (\bar{k}_s - \bar{k}_o) \quad (3)$$

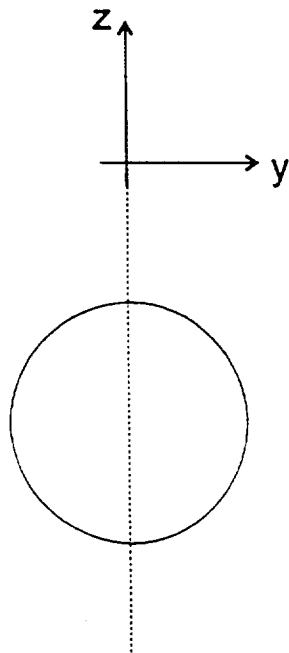
and hence, in the jet core:

$$I = \rho \int_{f=-\infty}^{f=\infty} [R^*(f_0 + \Delta f, \rho, T, \theta)] [P_{filter}(f_0)] df \quad (4)$$

If the density and temperature are assumed constant across the visualized plane, then:

$$\rho^* = \frac{\rho}{\rho_{\infty}} = 1.0 \quad (5)$$

$$\frac{I}{I_{\infty}}(\Delta f) = \frac{\int_{-\infty}^{\infty} R^*(f + \Delta f) P_{filter}(f) df}{\int_{-\infty}^{\infty} R^*(f) P_{filter}(f) df} \quad (6)$$



Assume: $U(y) = U(-y)$
 $V(y) = -V(-y)$
 $\rho(y, z) = \text{constant}$
 $T(y, z) = \text{constant}$

To obtain velocity data from a single averaged FRS image of a jet without tabs, the above assumptions were made.

Spectral Characteristics For the filter and ambient Rayleigh scattering

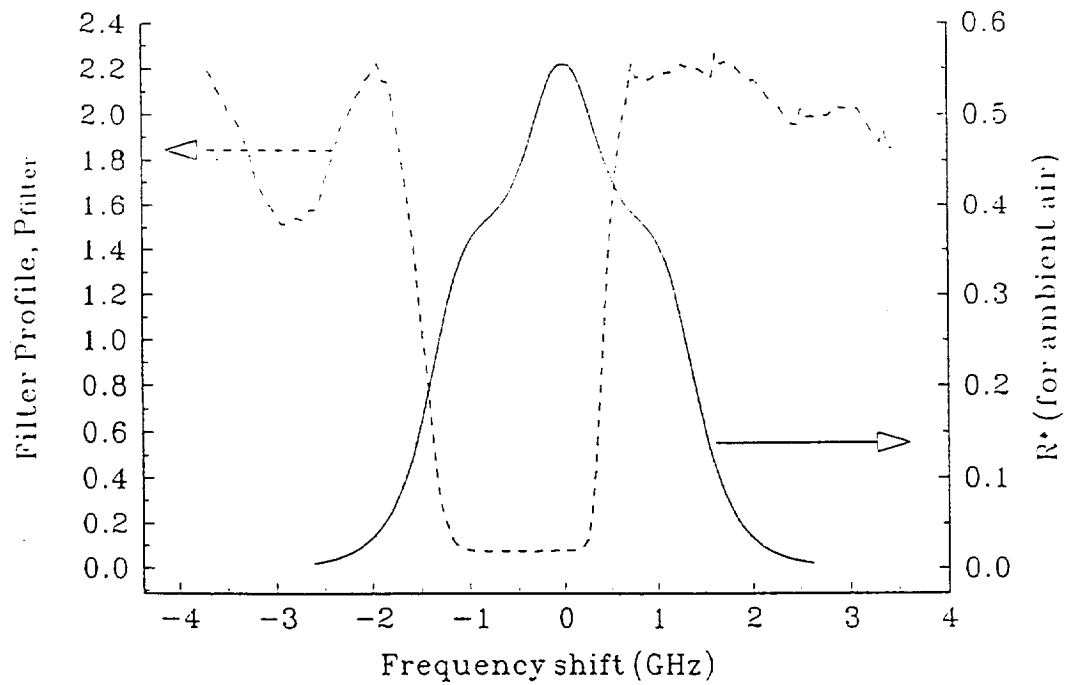


Figure 9. Spectral characteristics of the optical filter (dashed line) and the ambient scattering media (solid line). Zero frequency shift refers to the incident laser frequency.

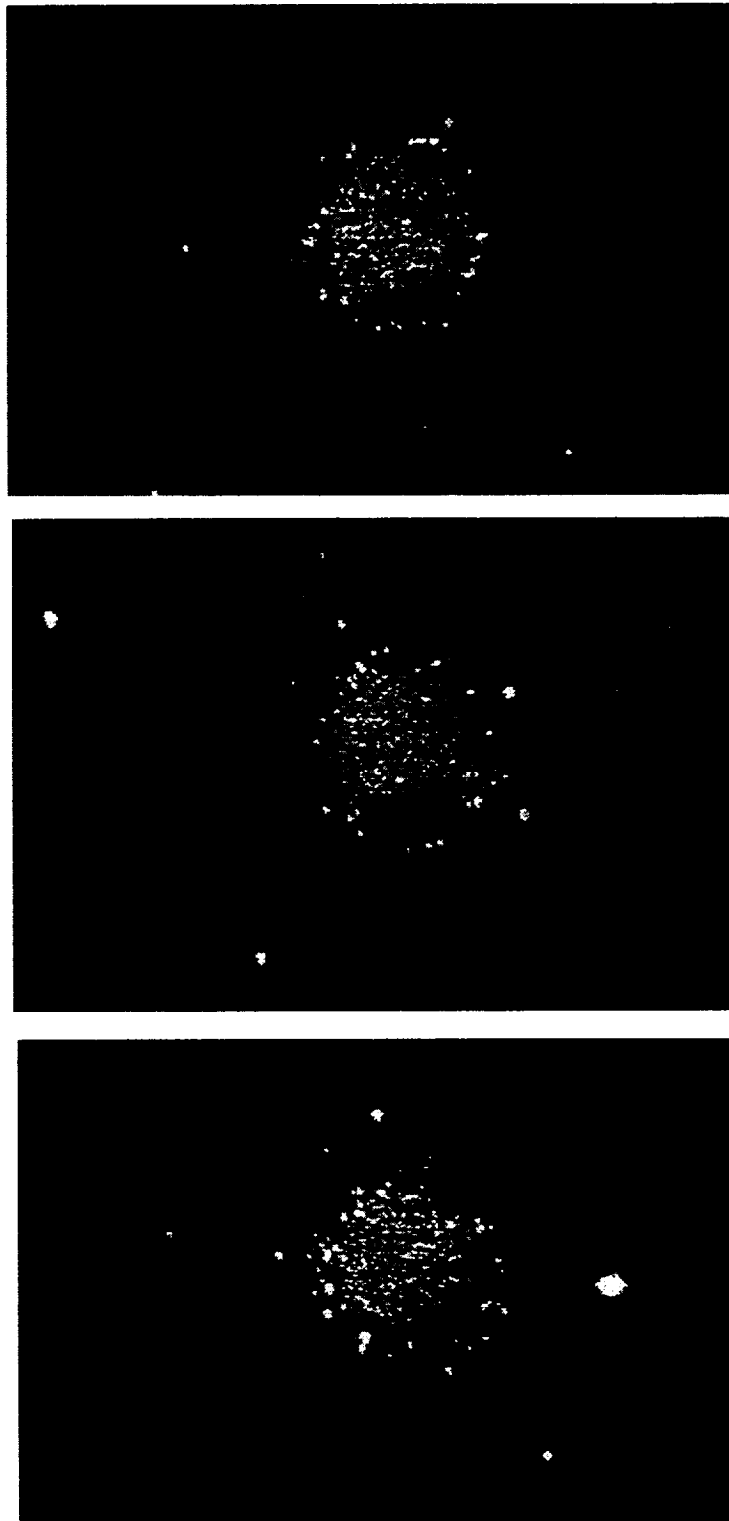


Figure 10. Three typical instantaneous filtered Rayleigh scattering images of a perfectly expanded, isothermal Mach 2 jet without tabs.

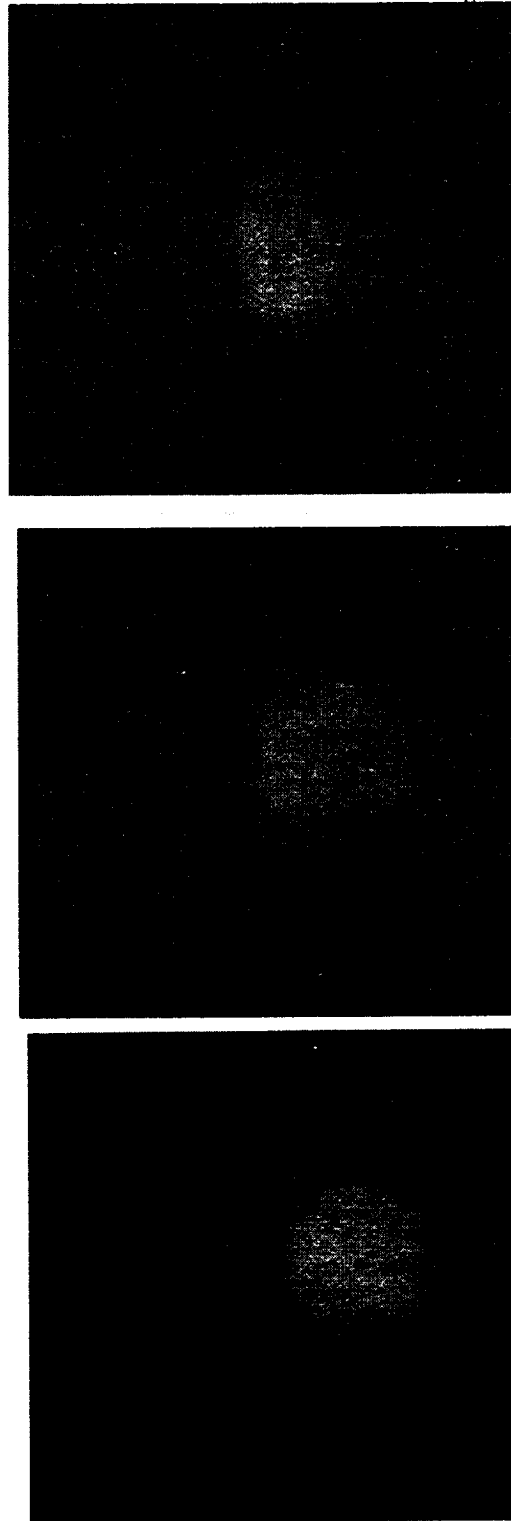


Figure 11. Post-processed, average images of filtered Rayleigh scattering for perfectly expanded, isothermal (a) Mach 1.0, (b) Mach 1.5, and (c) Mach 2.0 jets without tabs taken at $x/D=3$ for each case.

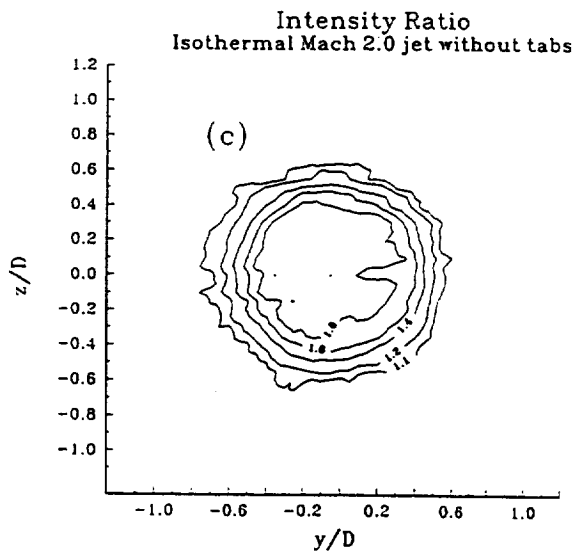
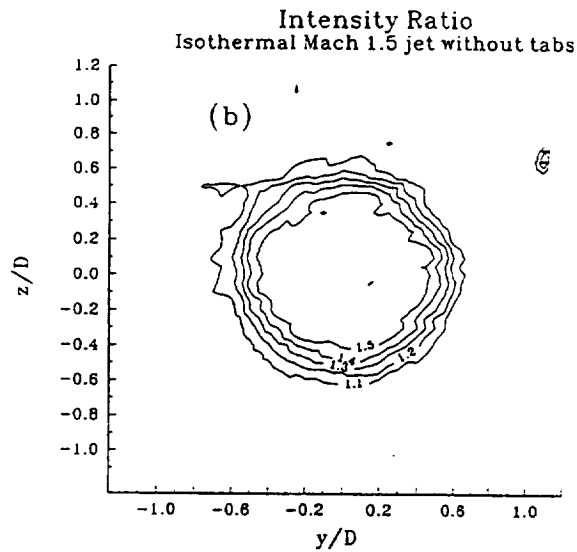
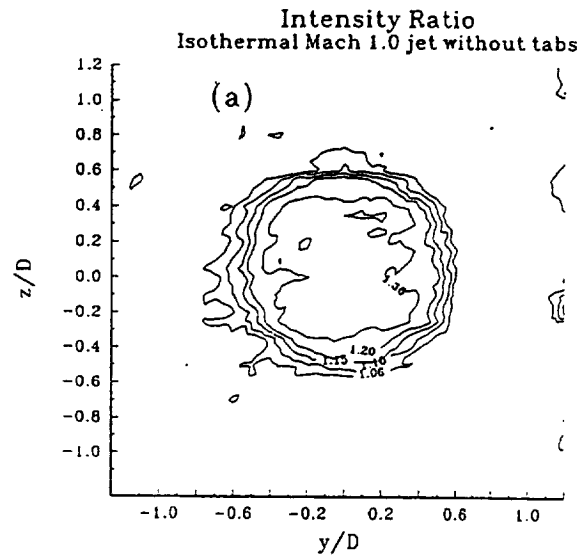
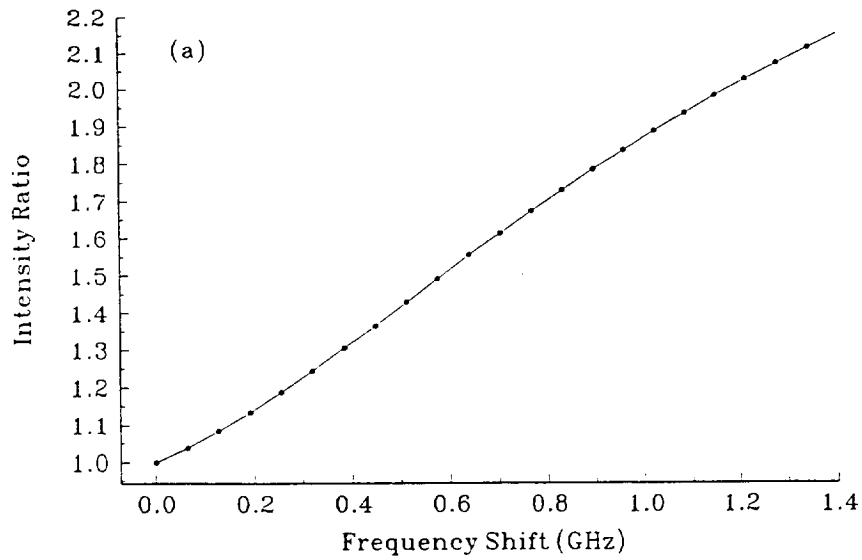


Figure 12. Intensity ratios from FRS for isothermal jets without tabs for (a) Mach 1.0, (b) Mach 1.5, and (c) Mach 2.0.

Intensity Ratio as a Function of Frequency Shift For isothermal no-tab cases



Frequency Shift as a Function of Intensity Ratio For isothermal no-tab cases

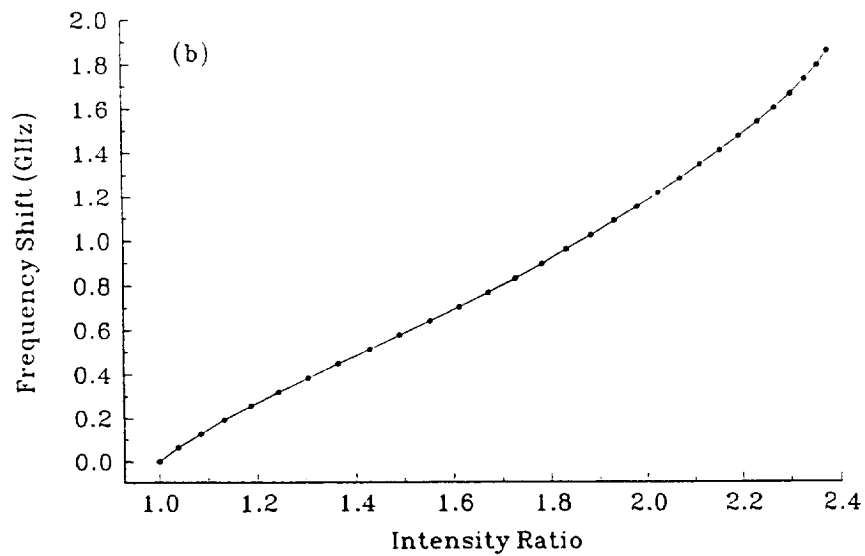


Figure 13. Relationship between intensity ratio and velocity for jets without tabs. In (a) the intensity ratio is calculated as a function of frequency shift for the given Rayleigh scattering spectra. This is then used for calibration to find velocities, shown in (b) for clarity.

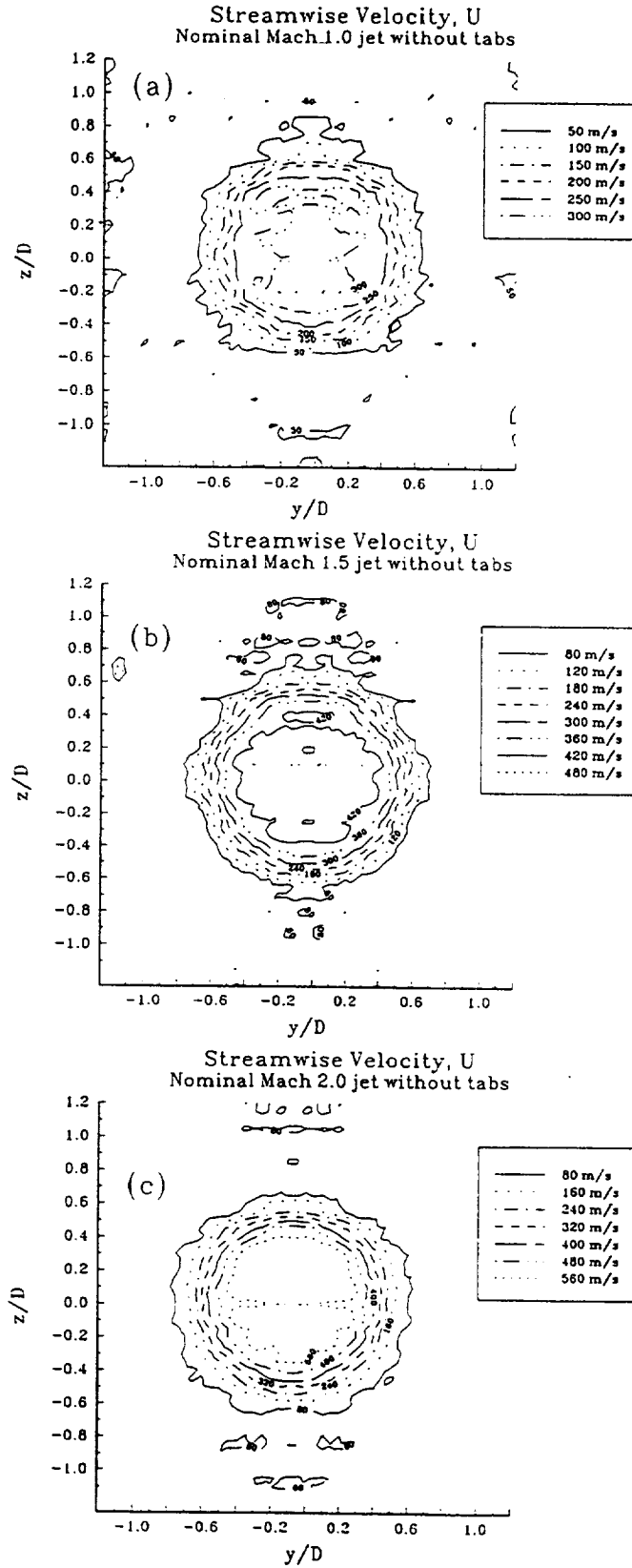
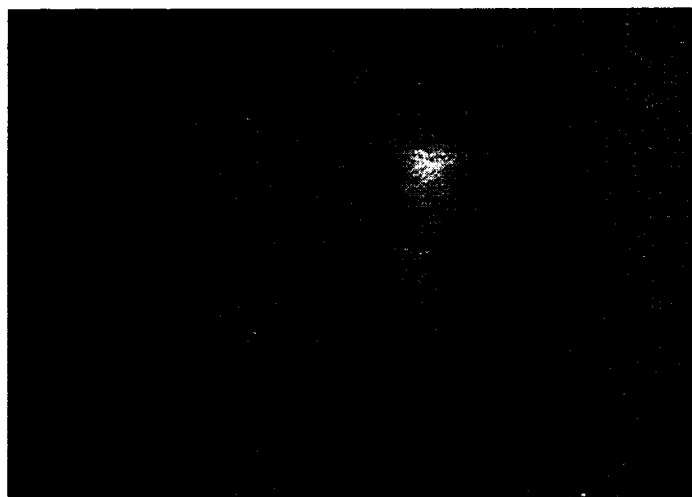
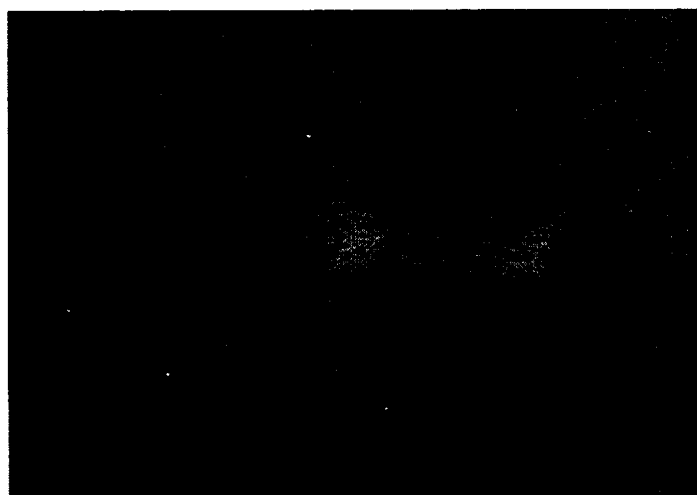
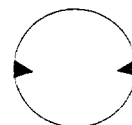


Figure 14. Streamwise velocity contours from FRS for isothermal jets without tabs for (a) Mach 1.0, (b) Mach 1.5, and (c) Mach 2.0.



(a)



(b)

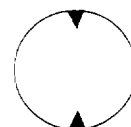


Figure 15. Post-processed average filtered Rayleigh scattering images of a Mach 1.5 jet with two delta tabs. In (a) the tabs are along the horizontal axis, and in (b) the tabs are along the vertical axis.

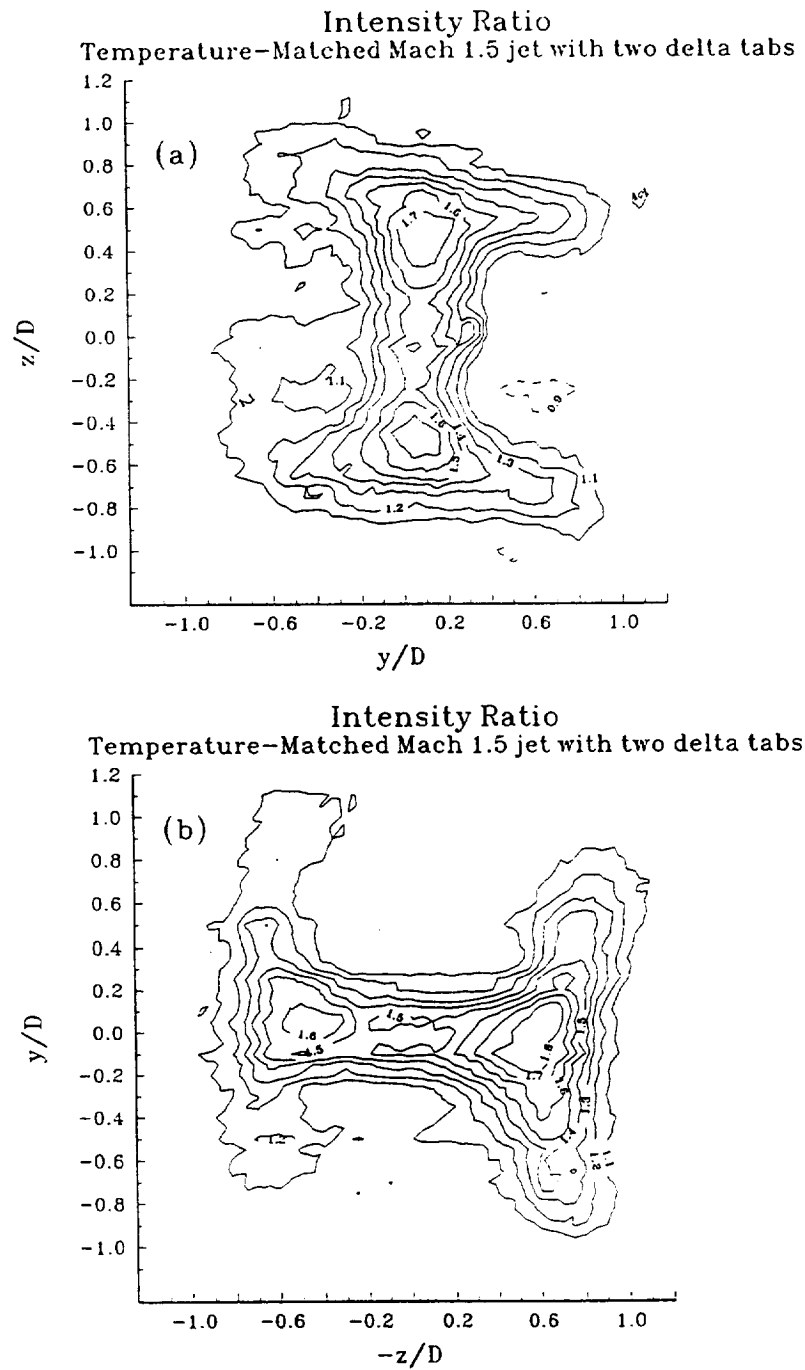
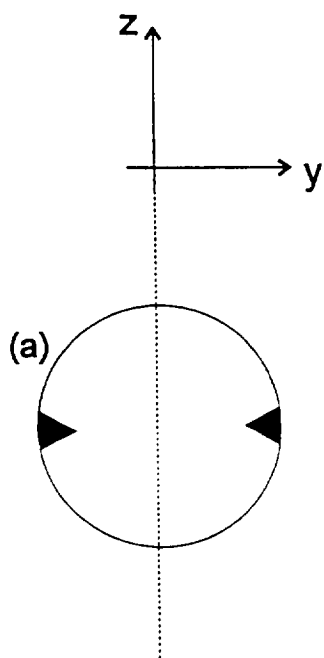
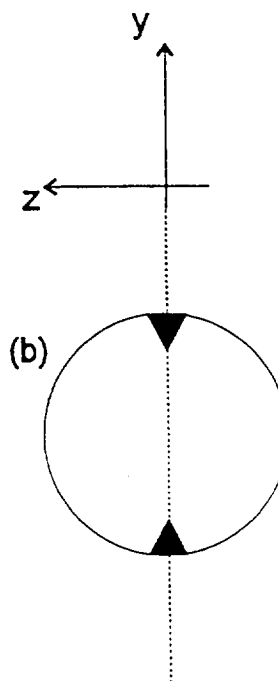


Figure 16. Intensity ratios for temperature-matched Mach 1.5 jets.
Tab orientation corresponds directly to Fig. 15.



Assume: $U(y) = U(-y)$
 $V(y) = -V(-y)$
 $\rho(y) = \rho(-y)$
 $T(y) = T(-y)$



Assume: $U(z) = U(-z)$
 $W(z) = -W(-z)$
 $\rho(z) = \rho(-z)$
 $T(z) = T(-z)$

To obtain quantitative data from a single averaged FRS image for a jet with two delta tabs, the above assumptions were made for the respective cases.

How can the intensity ratios be related to properties of the jet with tabs?

$$\frac{I}{I_{\infty}} = \frac{\rho}{\rho_{\infty}} * D[(k_s - k_{\rho}) \cdot \bar{V}] * E\left(\frac{\rho}{\rho_{\infty}}, \frac{T}{T_{\infty}}, \bar{V}\right) \quad (5)$$

The function term D is associated with the Doppler shift. The term E accounts for variations in the shape of the Rayleigh scattering signal.

Assuming only minor effects to changes in the scattering profile (i.e. E = 1.0) and assuming symmetry, tab configuration (a) yields:

$$\left(\frac{I}{I_{\infty}}\right)_{y>0} + \left(\frac{I}{I_{\infty}}\right)_{y<0} = \rho^* * \left[2 + 1.82 * f(U)\right] \quad (7)$$

$$\left(\frac{I}{I_{\infty}}\right)_{y>0} - \left(\frac{I}{I_{\infty}}\right)_{y<0} = \rho^* * \left[2.82 * f(V)\right] \quad (8)$$

and tab configuration (b) yields:

$$\left(\frac{I}{I_{\infty}}\right)_{z>0} + \left(\frac{I}{I_{\infty}}\right)_{z<0} = \rho^* * \left[2 + 1.82 * f(U)\right] \quad (9)$$

$$\left(\frac{I}{I_{\infty}}\right)_{z>0} - \left(\frac{I}{I_{\infty}}\right)_{z<0} = \rho^* * \left[2.82 * f(W)\right] \quad (10)$$

with f(U), f(V) and f(W) being taken from linear approximations of frequency (and hence velocity) vs. intensity ratio.

Scattering Half-Profiles For Constant Light Vector

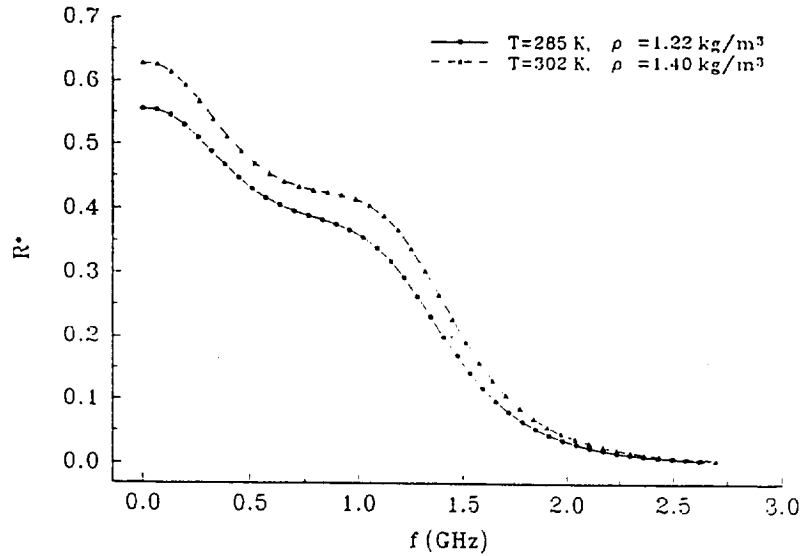


Figure 17. Comparison of the scattering half-profiles for air of the two thermodynamic states indicated. The higher density and temperature condition is reasoned to be "worst-case" for the Mach 1.5 delta tab case.

$\rho^*\{1+f(U)\}$ comparison Error estimation for Mach 1.5 delta tab cases

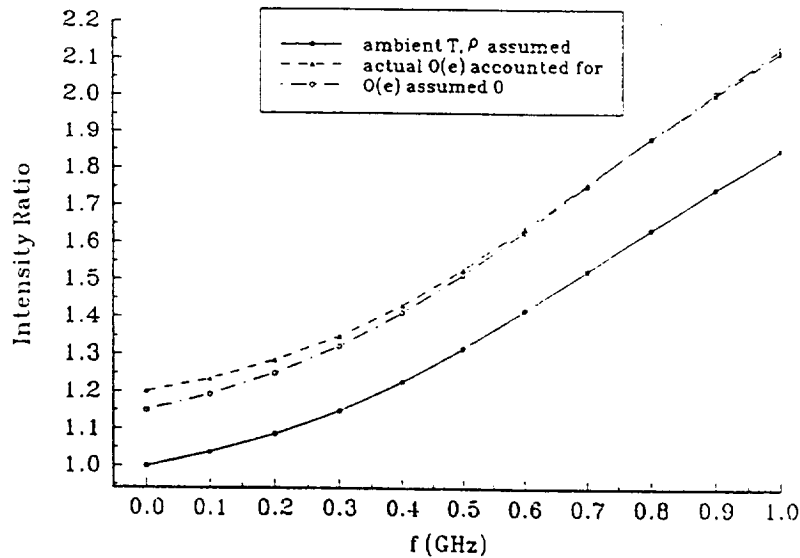


Figure 18. Assessment of the applicability of Eqn. 3 to the intensity ratio for the Mach 1.5 delta tab case.

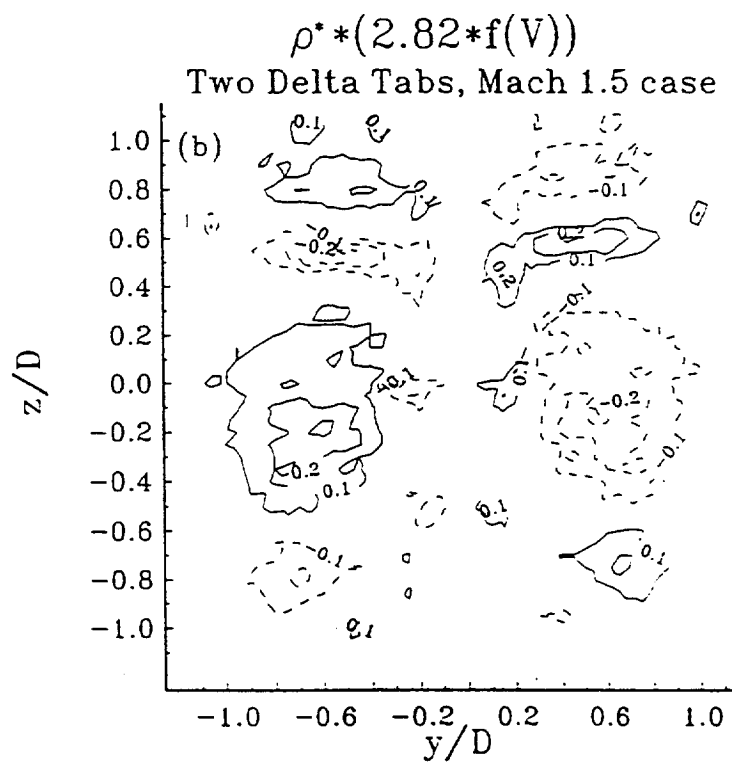
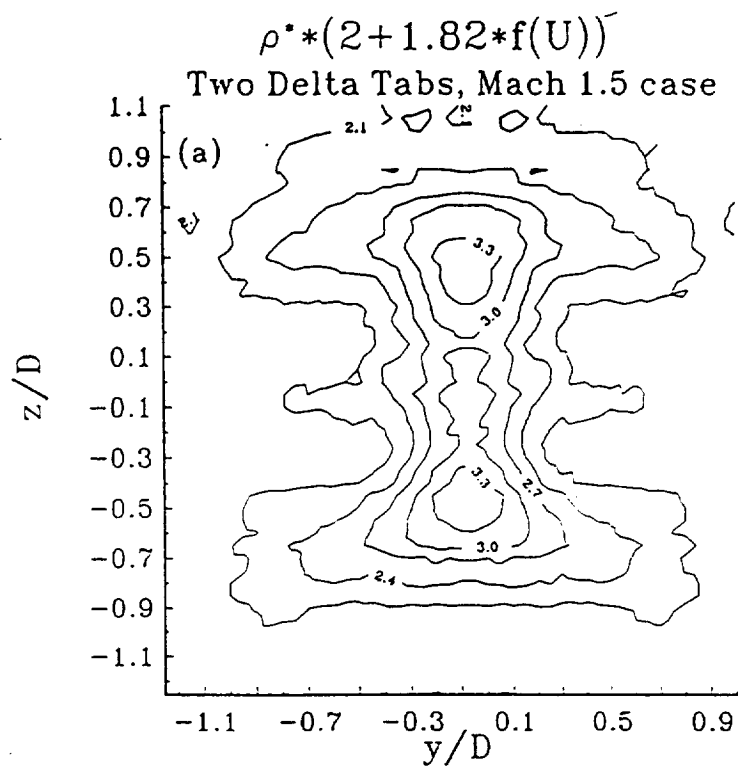


Figure 19. Quantitative values from FRS for a temperature-matched Mach 1.5 jet with two delta tabs. Tabs were placed along the y-axis.

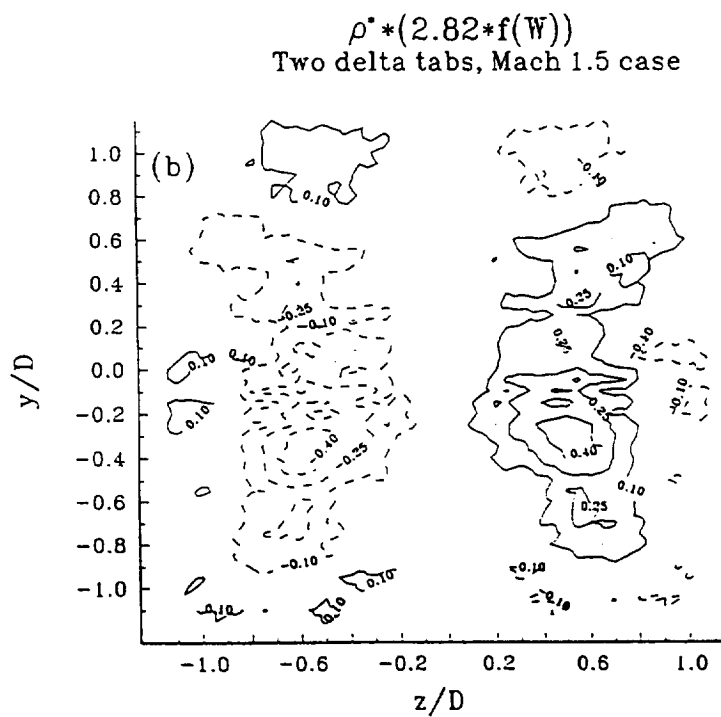
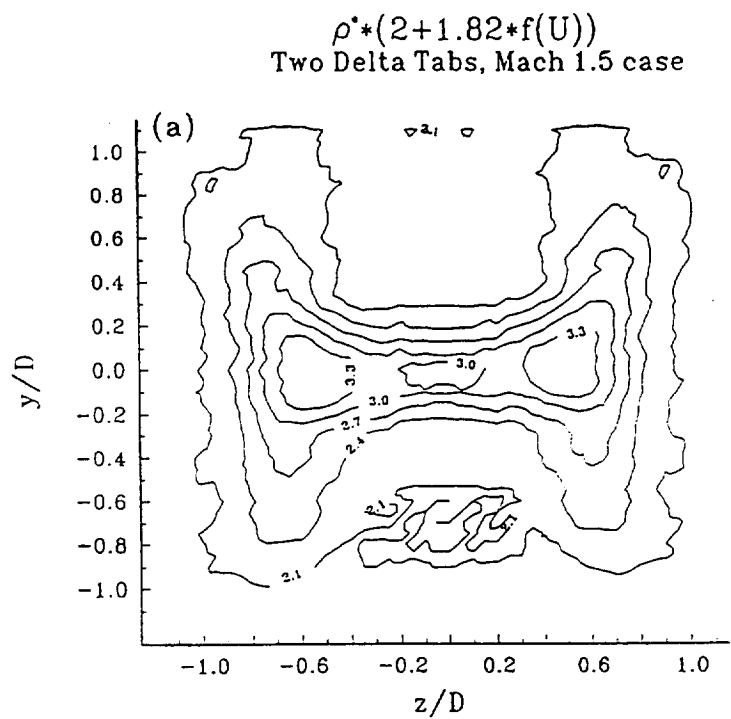
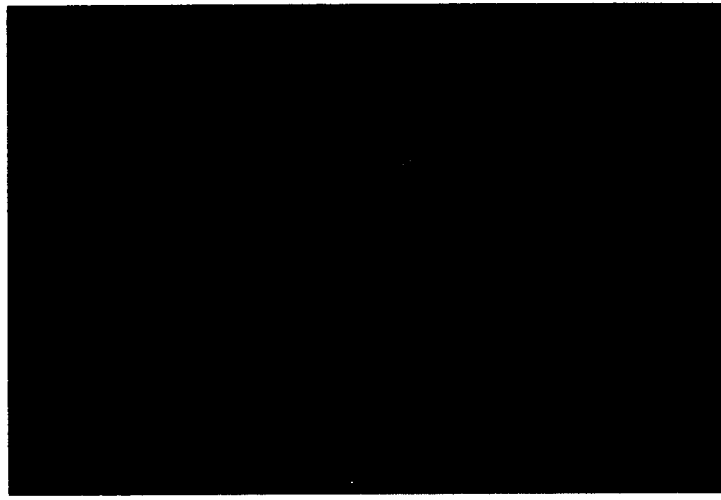
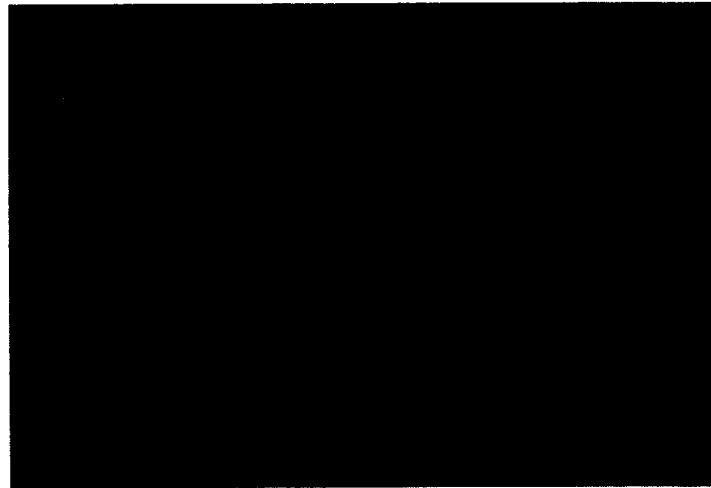
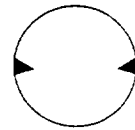


Figure 20. Quantitative values from FRS for a temperature-matched Mach 1.5 jet with two delta tabs. Tabs were placed along the y-axis.



(a)



(b)

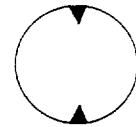


Figure 21. Post-processed average filtered Rayleigh scattering images of a Mach 2.0 jet with two delta tabs. In (a) the tabs are along the horizontal axis, and in (b) the tabs are along the vertical axis.

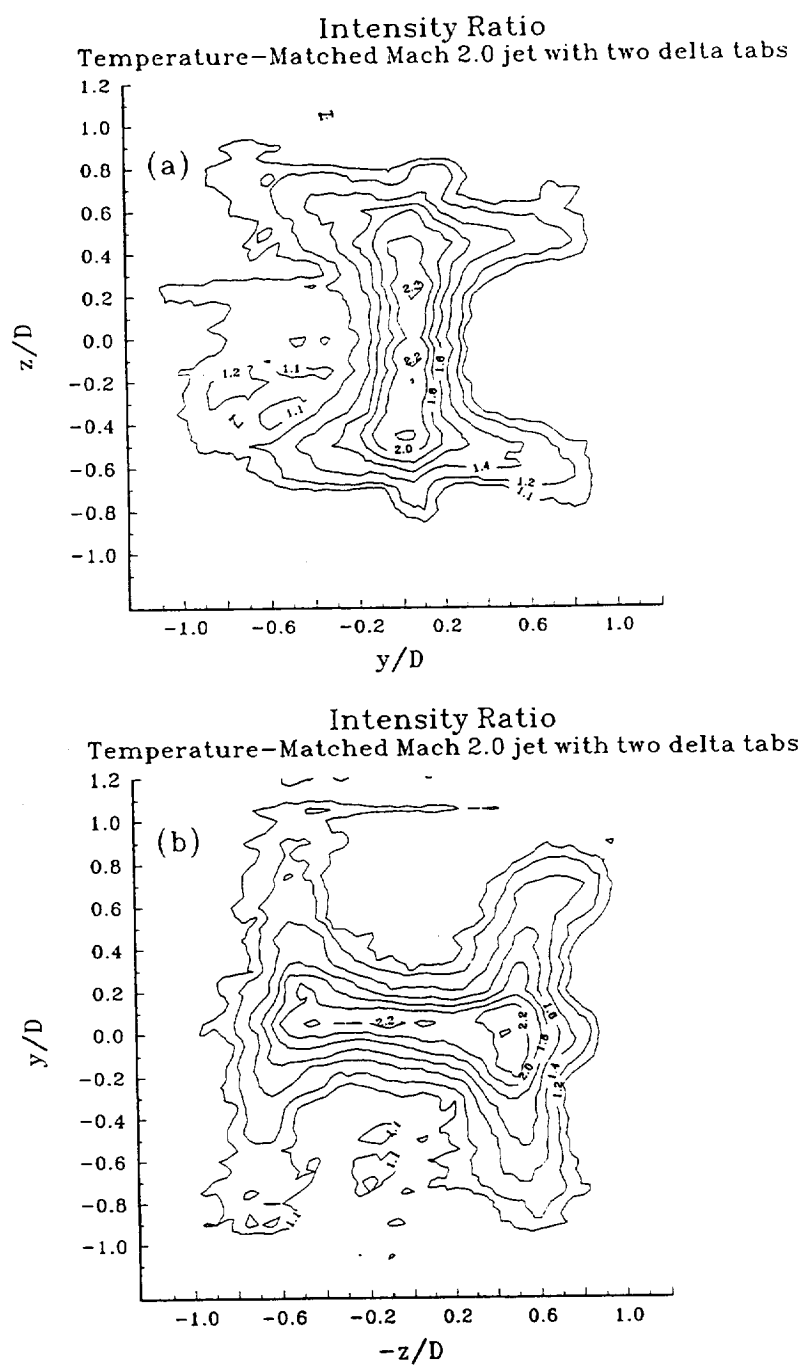


Figure 22. Intensity ratios for temperature-matched Mach 2.0 jets. Tab orientation corresponds directly to Fig. 21.

